Impact of Daily Melt and Freeze Patterns on Sea Ice Large Scale Roughness Features Extraction

Eric Hudier and Jean-Sébastien Gosselin
University of Quebec
Canada

1. Introduction

Improvement of large scale models developed to study the impacts of global changes in polar regions requires a better knowledge of the variability of the different parameters that control fluid dynamics and thermodynamics budgets at the interfaces. In the part of a fluid influenced by the presence of a solid interface, surface roughness is one of the key parameters that control momentum as much as heat (or salts at the ice-water interface) vertical exchanges through the boundary layer. This, in turn, makes roughness a data of primary importance when coupling ocean and atmosphere.
First year sea ice is characterized by large scale roughness features resulting from the accumulation of ice blocks that are piled above and below the surface under the compression and shear stresses induced by winds and currents. They develop linear sinuous features several hundred meters in length which on satellite images draw a network of bright structures. When illuminated by a SAR beam, the orientation variability of ice block faces in ridges increases the probability to receive an enhanced signal resulting from specular reflection on point sources. It follows that conditions that enhance specular reflection over diffuse scattering translate into a better resolution of the ridge network. This is mostly achieved at spring, when, with the snow wetness content increasing, the penetration depth into snow and ice becomes negligible. It has been observed that overnight wetness changes may cause strong resolution contrast on the ridge network. Late in the afternoon, increased wetness and the presence of a liquid film on ice and snow surfaces results in an increased forward scattering on most surfaces and an improved resolution of the pressure ridge network. On the contrary, on morning the reduced wetness allows some volume scattering to occur in the snow surface layer causing an increased diffused scattering that tends to reduce the backscattered signal from ridges and increase the signal from flat ice surfaces away from ridges.
In addition, with coherent imaging systems such as SAR, multiplicative random noise can combine to generate a signal strong enough to partly mask large roughness features signature. The speckle issue is for ridges of utmost importance. Extending only over several meters

Based on "Diurnal SAR variability due to ice and snow air interface wetness overnight changes.", by Hudier E., J-S. Gosselin & D. Febres, which appeared in the *Proceedings of the IGARSS, Barcelona 23-27 july 2007*.

across, ridges are best resolved at the highest available resolution. However, the reduction of speckle is first achieved through simultaneous processing of multiple looks at the expense of the spatial resolution. In fact, any attempt at getting information on ridges is hindered by the difficulties at extracting the very location of individual ridges out of a speckled image.
As a consequence, improving roughness extraction techniques requires to thoroughly understand and differentiate the physics behind signal coherence. In this chapter we will review the geophysical parameters that enhance the detection of the specular coherent component backscattered from ridges. In the conclusion we will review speckle properties emphasizing the physics differences between coherent summation and specular coherence as a mean to filter speckle from polarimetric SAR and improve pressure ridge resolution.

2. Background

The snow cover is an important component of the ice-atmosphere interface. It is known to accumulate in the wake of ridges creating mesoscale surface roughness features (Déry & Yau, 2001; Gallée et al, 2001). Whereas, during the winter season, the snow cover is mostly transparent to microwaves (Garity et al, 1990), at spring, the solar radiation and temperature changes cause the metamorphosis of snow crystals which in turn reduce the penetration depth and translate into volume scattering (Barber et al, 1998). Later on, as the snow wetness content increases, the dielectric properties changes of the wet snow medium reduce furthermore the penetration depth of radar electromagnetic waves and eventually turn the snow surface into an opaque medium (Koskinen, 2001; Barber et al, 1998).
At the beginning of the melt season, pressure ridges are mostly enveloped or coated with snow. As volume scattering still dominates, up to 4 % of volumetric wetness, (Koskinen, 2001; Guneriussen, 1997), they get drowned by the signal component back-scattered by is the snow layer and, as a consequence, are not well delineated on satellite images.

Between 5 and 8% humidity, surface scattering becomes the main component of the received signal and adds surface slope as a major factor in the analysis of microwave imagery (Hallikainen & Winebrenner, 1992). More exactly, the parameter to consider is the actual angle that the radar incident beam makes with the normal to snow or ice surfaces. After Gohin et al. (1994), and Lewis et al. (1994), the back-scattered intensity σ_0 (in decibels) is well described by a linear function of θ, the angle made between the normal to the iceor snow interface and the radar incident beam:

$$\sigma_0(\theta) = \sigma_0(0°) + C_i\,\theta \tag{1}$$

Kim et al. (1984) showed that σ_0 (0°) and the slope C_i are characteristic of the surface roughness. In the case of electromagnetically smooth surfaces, such as an ice block in a pressure ridge, the radar return is large at normal incidence and σ_0 decreases rapidly with θ as most of the radar energy scatters forward. In contrast, rough surfaces show a reduced dependence with θ.
In addition, at spring, the orientation of snow and ice surfaces relative to sun rays can, depending on solar irradiation intensity, translate into a variability in surface snow wetness, eventually the development of a film of liquid water on ice surfaces and, as irradiance decreases over the day, the re-crystallization and build-up of frost flower structures where liquid films formed on ice blocks. Thermodynamically, the snow ice medium is during this

period of the year at the fresh water freezing point (Gow & Tucker III, 1990; Wadhams, 2002; Petrenko & Whitworth, 1999). While within the snow layer the heat budget is only balanced by melt or freezing of ice crystals or interstitial liquid water, at the air snow interface, evaporation comes into play to remove or add heat. As a consequence, while the water content within the snow layer changes slowly, at the air interface evaporation can quickly shift the surface temperature below freezing turning a thin layer of snow into a dry medium then allowing microwaves to penetrate and generate volume scattering.
Beside the incident angle, the most important parameter when analyzing SAR images is the surface roughness of the snow-air interface (Ulaby et al, 1990; Fung, 1994). Fundamentally, the electromagnetic wave interaction with a snow surface is determined by the scattering efficiency of surface roughness *rms* and correlation height. The transition from electromagnetically smooth to rough surface depends on an arbitrary criterion that is proportional to $[\lambda/\cos\theta]$, where λ is the radar wavelength and θ the radar incident angle. On terrains that offer surface slope variability such as ice block faces or snow cover surfaces, θ must be seen as the local incident angle relative to a given area. The proportionality factors vary from 1/8 (the Rayleigh criterion) to 1/32 (the Fraunhofer criterion). It results that at normal incidence ($\theta=0°$) a surface roughness *rms* between 0.15 cm and 0.6 cm causes a transition from smooth to rough surface. On ice surfaces a thin film of water, such as observed at spring during sunny afternoons, turn ridge blocks into specular reflectors. This allows for an increased contrast between ridges and the snow covered background due to the variability in surface orientations and occurrence of multiple reflection on several faces in ridges (Hudier, 2006; Carlstrom & Ulander, 1995). On the other hand, it can also cause an enhanced forward scattering on snow surfaces, generating dark stripes or low backscattering areas where surface slopes cause the SAR incident beam to reach the snow interface at a large angle.

3. Field site and image processing.

Images analyzed in this paper were recorded as part of a field work conducted on the east coast of the Hudson Bay offshore of Kuujjuarapik, Quebec, Canada (Figure 1). This area is covered with a first year landfast sea ice about 1m30 to 1m60 thick. By mid-April the first signs of melt can be observed with an increase of snow wetness. By mid-May, most of the snow is melted away with some left where sheltered from sun rays on the north side of ridges. Figure 2 shows an aerial photograph of the study area.

Fig. 1. Geographic location of the site where field works were done (white star).

Fig. 2. Early May picture of the ice sheet offshore Kuujjuarapik, Quebec, Canada.

Overall thirteen Radarsat-1 SAR fine beam mode scenes were processed "table I". In its fine beam mode, the Radarsat antenna looks to the right of the spacecraft at an angle between 35° and 49° with a resolution 8-9 m and a swath area of 57x50 km. The average local overpass times were 5:30 am (descending) and 4:57 pm (ascending). Processing of the data were done using ENVI-6.2 software. Fields works were carried out offshore of Kuujjuarapik on the East coast of the Hudson Bay. Detailed information about data collection and image processing can be found in Hudier (2006).

From the data set listed below, 7 images (in bold) were recorded after wet conditions were observed. All images recorded early in the morning were recorded after a night below freezing. Qualitative analysis shows that morning images offer a poor resolution of the ridge network. In all instances afternoon images offer a better resolution. Isolating areas that could be identified as ridges and areas that didn't show any sign of a ridge, we computed the average change in the backscattered signal between morning and afternoon images. Our results show a 4 dB decrease in ridged areas with a 5.5 dB std. In areas away from ridges an increase of 1.9 dB with a 2.5 dB std was computed.

Recording date	Mode	Incident angle	Orbit
April 23, 1997	F2	40.3-42.5	Descending
May 10, 1997	**F1**	**36.8-39.9**	**Descending**
April 04, 1998	F1	36.8-39.9	Ascending
April 11, 1998	F1	36.8-39.9	Descending
April 28, 1998	**F1**	**36.8-39.9**	**Ascending**
May 05, 1998	**F1**	**36.8-39.9**	**Descending**
March 26, 2001	F1	36.8-39.9	Descending
April 26, 2001	**F2**	**40.3-42.5**	**Descending**
April 29, 2001	**F3**	**41.1-43.1**	**Ascending**
April 15, 2005	F1	36.8-39.9	Ascending
April 22, 2005	**F1**	**36.8-39.9**	**Descending**
April 25, 2005	F4	42.3-44.5	Ascending
May 02, 2005	**F2**	**40.3-42.5**	**Ascending**

Table 1. SAR images acquisition

4. Low back-scattering areas paralleling pressure ridges.

4.1 Methods

Data used in this research work were collected over four field experiments: 1997, 1998, 2001 and 2005. Field work was done from mid-April to mid-May which covers the melt initiation period for this region of the bay. A detailed survey of the snow layer and ridge features was performed systematically along a total of eight transects which start and end points were geo-referenced. 87 measurement sites were selected along these transects to sample a range of ridge orientations relative to SAR incident beams. The mapping of the snow layer morphology included: structure orientation, slope, size, lateral extension of the structures relatively to the ridge, and normal vs. satellite incidence angle. Ridge characteristics measurements included: height, width, block size and distribution. In order to study the relation between surface orientation and the backscattering reduction from these regions, we measured the angle between the radar incident beam's orientation and the perpendicular to the slope. At each sampling location, data were collected along 4 transects parallel to ridge axes at distances of 5, 10, 15 and 20 meters. Measurements were made at regular intervals along the different transects. Also, ridge blocks surface characteristics were documented as a function of face orientations. In addition, snow temperature and wetness were measured using a thermocouple sensor and a snow fork (dielectric measurement device). These last data were collected for each SAR scene on the day and time (+/- 30 minutes) the images were recorded.

Selected sites were first extracted from the available set of images and sampled areas located. Backscattering data were then computed over a set of 3 pixels wide strips oriented parallel to ridge axes, a first strip localized over the ridge itself, and a second next to it in the area of reduced backscattering. This operation was performed manually by moving a test strip across the ridge in order to localize the areas of maximum (the ridge) and minimum backscattering. Backscattering statistics and the distance between the areas of reduced backscattering and the adjacent ridge were then computed. It must be underlined that for a site to be classified as having a "dark band" there had to be continuity between the band of minimum backscattering and the middle of the adjacent floe.

4.2 Low backscattering regions associated with ridges.

As anticipated, areas of reduced backscattering were observed paralleling ridges (Figure 3). This result confirms previous observations. We also confirmed that these dark structures get more contrasted as the spring melt goes on.

Overall, they were observed on 61% , 53 out of 87, of our sample locations. However, in most of the 53 sites they showed up only on images recorded later at spring (table 2). In the case of 3 images recorded before mid-April, no such structures were spotted. This period of the season is more typical of the winter conditions. The maximum snow wetness amounted then to 0.8 % in which conditions volume scattering and other boundary surface scattering become important. Snow wetness was observed to be highly variable depending on the sampling point location. Surfaces perpendicular to sun rays display the highest surface wetness content, which was measured in the first 5 mm of the snow layer. However, when sampling a thicker layer (10cm) the snow drift geometry becomes a factor. We observed a lower wetness content on crests and maximums in troughs. Table 3 summarizes the average backscattering value computed from ridges, dark band areas and on floes away from sampled ridges.

Fig. 3. Reduced back-scattering in areas bordering pressure ridges on a RadarSAT 1 image of a first year sea ice.

Recording date	Nb of test sites	Sites with dark bands
April 23, 1997	12	4
May 10, 1997		7
April 04, 1998	23	0
April 11, 1998		0
April 28, 1998		14
May 05, 1998		14
March 26, 2001	20	0
April 26, 2001		12
April 29, 2001		14
April 15, 2005	32	15
April 22, 2005		17
April 25, 2005		17
May 02, 2005		16

Table 2. Percentage of sampled locations where dark bands were observed.

σ0 (dB)	Average	Average distance to ridge
Ice floes away from ridges	-16.2	
Bright ridges	-13.5	
Dark strip	- 17.7	22 (m)

Table 3. First year sea ice signatures

In the lee of pressure ridges snow accumulates behind obstacles to form linear features oriented after the wind that developed them. It creates a wave pattern with crests heights tapering away from ridges. These structures offer a wide range of surface slopes that differentiates this region from the rest of the ice floe. As underlined by data summarized in table 4, in cases where physical obstacles may generate slope patterns, pressure ridges can not only draw a network of bright linear features but also a network of dark bands parallel to these bright features. This also underlines how, when spring melt turns the snow cover into an opaque medium, snow slopes and orientation relative to the sun and the satellite beam can be as an important parameter as surface roughness.

σ0 (dB)	Slope average	Std
Ice floes away from ridges	38°	15°
Ridge vicinity where σ0 is reduced	72°	28°
Ridge vicinity where σ0 is not reduced	44°	35°

Table 4. Snow surface slope characteristics in three regions: (1) away from ridge influence, (2) in the vicinity of the ridge where reduced backscattering was measured and, (3) in the vicinity of the ridge where no-reduction of the backscattering intensity was measured.

5. Resolution variability due to overnight wetness changes.

5.1 Overnight resolution loss

Figure 4 and 5 give an example of resolution variability on two ridge networks. In the 2 situations the day prior to the image recording was sunny and warm, liquid films were observed on snow and ice surfaces during mid-afternoons with water contents over 8% in the first centimeter of the snow layer. Figure 4 was recorded at 4 pm with temperatures close to the air temperature peak for the day (Figure 6). In the situation pictured on figure 5, the image was recorded at 4 am on the morning, after the night temperature went down below freezing (Figure 7). At that time, surface wetness was measured at 3.1% and frost flower observed where liquid films were spotted the previous afternoon. Similar diurnal "patterns of daily melt and nightly freeze" were also reported by Ashcraft and Long (2005) to cause a strong increase of the absorption coefficient of the snow due to the introduction of liquid water into the snowpack.

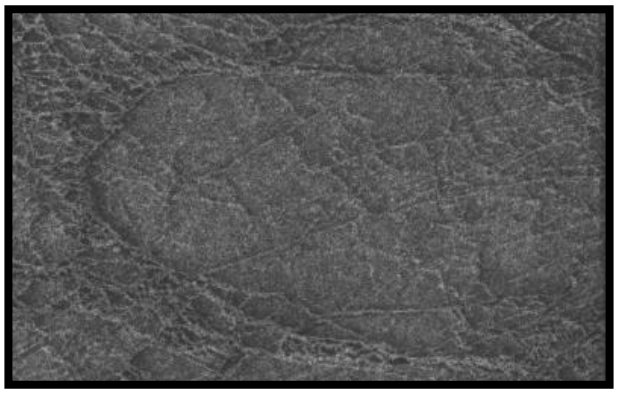

Fig. 4. SAR image recorded at 4 pm after a warm and sunny day, East coast of the Hudson bay, Canada.

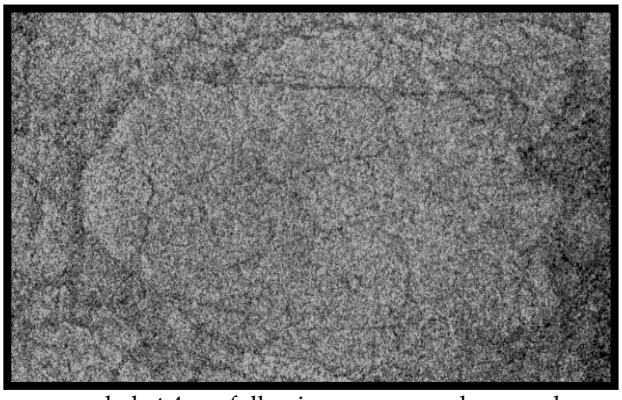

Fig. 5. SAR image recorded at 4 am following a warm and sunny day, and after a night with temperatures below freezing, East coast of the Hudson bay, Canada.

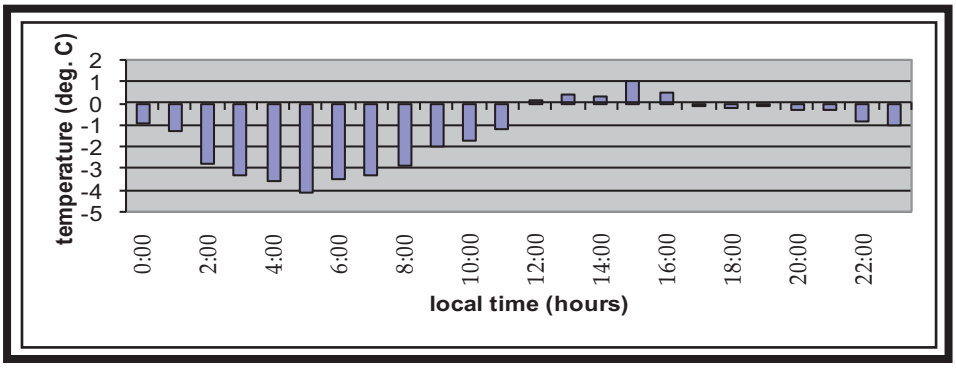

Fig. 6. Temperatures recorded at the meteorological station of Kuujjuarapik, Quebec, Canada, on the day the image displayed on figure 2 was recorded.

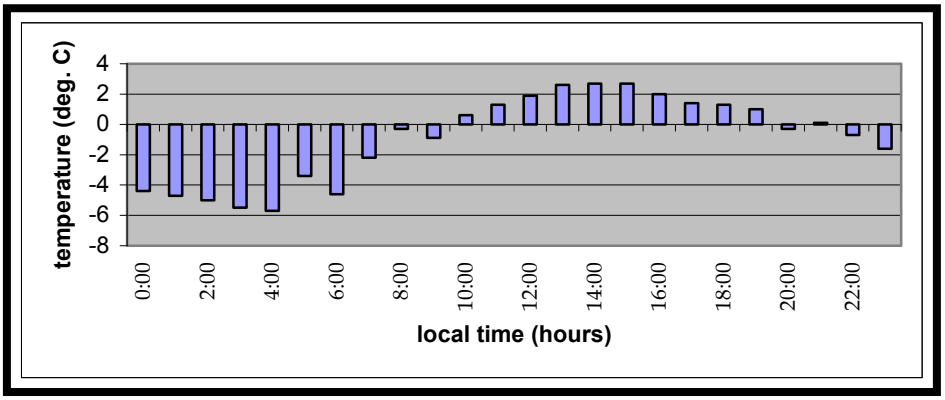

Fig. 7. Temperatures recorded at the meteorological station of Kuujjuarapik, Quebec, Canada, on the day the image displayed on figure 3 was recorded.

5.2 Field data and discussion

The wetness content was measured in the first centimetre of the snow cover and at 5 centimetres below the surface. At the end of the afternoon we observed a light dependence between surface wetness and the orientation of the surface slope relative to the zenith. As expected, surfaces subject to a higher irradiation showed a higher wetness content. In the first centimetre the wetness averaged 7.5 with a std of 2.1 at +/-30° from normal sun incidence and 6.3 with a std of 3 for larger incidences. At 5 cm from the surface, surface slope orientation does not show any significant influence on the water content. We measured an average 3.9 with a std of 2.1. Data collected at 4 am give wetness contents of 3.1 in the first centimetre with a std of 2.9 and no clear slope dependence. It is to be noted that a liquid film was observed on both on most ice and snow surfaces in sampling completed in the afternoon.

The reduced resolution on morning images is the result of two things. First a reduced backscattering in ridged areas and secondly an increased backscattering from areas away from ridges. This second phenomenon is well explained by an increased penetration depth and the resulting volume scattering due to a reduced wetness in the top layer and the metamorphosis of the snow cover that is associated the succession of thaw and freezing that occurs overnight (Barber et al., 1998).

In ridged areas, where some bare wet ice faces were observed mid-afternoon, all ice blocks faces were dry on morning. Besides, no "pure ice faces" were observed. Selected ice blocks sampled daily showed that where bare wet ice can be found at some point during the day, a thin layer of flower frost develops at night with measured *rms* values in and above the smooth to rough transition range for SAR Radarsat 1.

At spring, when the solar irradiation cycle causes diurnal temperatures to rise above freezing during the day and sink below freezing at night, our observations show a clear resolution difference between images recorded early in the morning and at the end of warm and sunny days. Wetness changes overnight are in the value range that causes the snow cover to become opaque to microwave lengths. During the day, the increase of the

absorption coefficient cause surface scattering to become dominant over volume scattering (Ulaby et al., 1990) and, therefore surface slope and roughness to control the microwave energy back-scattered toward the antenna. With the development of a liquid film on surfaces, microwaves do not penetrate anymore into snow or ice mediums, reflectivity increases and forward scattering occurs. As a consequence, all but the surfaces which lie almost at a right angle with the satellite beam return a weaker signal. As the probability that an ice surface may lie perpendicular to the incident SAR beam is much higher in ridges, this increased forward scattering on most surfaces results in an improved resolution of the pressure ridge network. As shown on figure 8, most ice blocks are enveloped in a thin layer composed of metamorphosed snow crystals, ice and air bubbles. With no porous medium

Fig. 8. Two ridges that gave similar backscattering intensity on the satellite image illustrated on figure 4. The probability density that an ice surface lies perpendicular to the incident ice beam increases with smaller ice blocks.

beneath, liquid water resulting from surface melt creates a continuous film that reduces surface roughness as well as increases its dielectric constant. Microwaves penetration is then negligible and most of the SAR beam energy reflected according to Snell's law. The development of a liquid film on ice blocks' faces turns each of them into an opaque electro-magnetically smooth surface which increases furthermore their brightness on satellite images.

During the night, temperature below freezing pumps heat out of the top layer of the snow cover causing wetness to drop. On morning, at the time the image illustrated on figure 5 was recorded, the reduced wetness content allows some volume scattering to occur in the snow surface layer to completely erase contrast between ridges and flat ice. In ridges, freezing removes the liquid film from ice block's faces turning them into an highly diffusive dry ice – snow crystals and air bubbles medium. This allows part of the microwave energy to penetrate into it causing a drop in the surface scattering component. Besides, some growth of snow flower crystals at the surface increases roughness to cause back-scattering from surfaces oriented perpendicularly to the incident SAR beam to drop furthermore. It should be observed that despite a loss in ridge resolution, some ridges remain visible (Figure 5) mainly because of the areas of reduced back-scattering as discussed in section 3.

6. Conclusion and polarimetric potential for ridge extraction

Results presented in section 4 and 5 underline the critical impact of wetness changes during spring time. With snow temperatures at the freezing point, any change in the snow-atmosphere heat flux initiates melt or freezing in the top layer of the snowpack. While, within the snowpack, water content undergoes only slight variations over a 24 hours period, snow crystals within the top layer can turn from wet to dry overnight. More importantly, where an ice surface is exposed to the atmosphere, melt and freezing cause the cyclic development of a liquid film and a re-crystallized highly diffusive dry layer of snow, ice and air bubbles. As liquid water is removed, part of the microwave energy penetrates into this layer to be absorbed and scattered. The fact that the ridge network can completely vanish overnight emphasizes the importance of specular reflection on electro-magnetically smooth surfaces for the extraction of ridges.

Surface roughness changes not only increase (or decrease) drastically the back-scattering from surfaces oriented perpendicularly to the SAR beam but also cause the back-scattered electromagnetic wave to be the result of an incoherent (or noncoherent) or coherent reflection. To explore furthermore the implications we need to clarify the concept of incoherence. In principle we measure the combined reflections from all scatterers within the scene which in term of physics is coherent summation. However, incoherence, in the literature, refers to the nature of the scene rather than to the physics of electro-magnetic waves. If the scene is viewed twice through the exact same geometry, the same speckle pattern should be observed (Raney, 1998). Conversely, due to the random distribution of individual scatterers, a slight change in the position of the satellite would give a totally different speckle pattern despite the fact that the statistics over the scene would remain unchanged. This is the incoherence nature of speckle which turns a mostly uniform area into a salt an pepper image. On the other hand, coherent specular reflection describes a highly correlated phase structure within part of a scene, which implies that multiple measurements from this same scene would reveal the presence of a specular reflector. This requires that the satellite position remains the same in order for the relative geometry of the SAR beam angle and target to be about the same.

Polarimetric SAR are systems that acquire two simultaneous images (HH and VV) of a same scene. While the geometry of the relative positions of the satellite and scene are unchanged, the physics of coherent summation from multiple scatterers implies that the two images would show a different speckle pattern. Conversely, the nature of specular coherent reflection implies that a specular reflector would be pinpointed on both images. It follows that the cross-correlation of single look HH and VV channels could help filter bright pixels generated by speckled coherent summation while revealing the pressure ridge network.

7. References

Ashcraft I.S. & Long D.G. (2005). Differentiation Between Melt and Freeze Stages of the Melt Cycle Using SSM/I Channel Ratios. *Geoscience and remote sensing IEEE Transactions*, vol. 43, No.6, pp.1317-1323.

Barber D.G., Fung A.K., Grenfell T.C., Nghiem S.V., Onstott R.G., Lytle V.I., Perovich D.K. & Gow A.J. (1998). The role of snow on microwave emission and scattering over first-year sea ice, *Geoscience and Remote Sensing, IEEE Transactions*, vol. 36, I.5, pp.1750-1763.

Carlstrom A. & Ulander L.M.H. (1995). Validation of backscatter models for level and deformed sea-ice in ERS-1 SAR images, *Int. J. Remote Sens*., V.16, No.17, pp.3245 – 3266.

Déry, S.J. and Yau M.K. (2001). Simulation of blowing snow in the Canadian Arctic using double moment model, *Boundary-Layer Meteorol*., 99, 297 – 316.

Fung A. (1994). Microwave scattering and emission models and their applications, *Artech House*, 573 p.

Gallée, H., Guyomarc'h, G & Brun, E. (2001). Impact of snow drift on the Antarctic ice sheet surface mass balance: possible sensitivity to snow-surface properties, *Boundary-Layer Meteorol*., 99,1-19.

Garrity C., Ramseier R.O. & Rubinstein I.G. (1990). Snow wetness and SSM/I brightness temperature for the Weddell Sea. *Proceedings of the IGARSS, 1990*, pp.1521-1524

Gohin F., A. Cavanié & R. Ezraty (1998). Evolution of the passive and active microwave signatures of a large sea ice feature during its 2½-year drift through the Arctic Ocean. *J. Geophys. Res.,* 103, 8177-8189.

Gow A.J. & Tucker III W.B. (1990). Sea Ice in the Polar Ocean, In: *Polar Oceanography, Part A, Physical Science,* Walker O. Smith Jr., (Ed.), 47-122, Academic Press, ISBN 0-12-653031-9, San Diego.

Guneriussen T. (1997). "Backscattering properties of a wet snow cover derived from DEM corrected ERS-1 SAR data", *Int. J. Remote Sensing*, Vol. 18, No. 2, pp. 375-392.

Hallikainen, M. & Winebrenner D. P. (1992), The Physical Basis for Sea Ice Remote Sensing. In: F.D. Carsey, Editor, *Geophysical Monograph* **vol. 68**, American Geophysical Union, Washington, pp. 29–46.

Hudier E. (2006). Low back-scattering bands paralleling pressure ridges on first year sea ice, *Proceedings of the IGARSS*, *2006*, Denver, pp.731-734, july 2006.

Kim Y.S., Moore R.K. & Onstott R.G. (1984). Theoretical and experimental study of radar backscatter from sea ice. *Remote Sensing Laboratory, Univ. Kansas Rept.,* RSL TR 331-337.

Koskinen J. (2001). Snow monitoring using microwave radars, *Thesis Doctor of Technology*, Helsinki University, 31p.

Lewis E.O., Livingstone C.E., Garrity C. & Rossiter J.R. (1994). Chapter 2: Properties of snow an ice, in *Remote Sesing of Sea Ice and Icebergs*, S.Haykin, E.O. Lewis, R.K. Raney and J.R. Rossiter (Ed.), John Wiley & Sons, Inc., 21-96.

Petrenko V.F. & Whitworth R.W. (1999). Physics of Ice. Oxford University Press, 373 p., ISBN 0-19-851895-1, New-York.

Raney R.K. (1998). Chapter 2: Radar fundamentals: Technical perspectives, in Principles and applications of imaging Radar; Manual of remote sensing Volume II, F.M. Henderson & A.J. Lewis (ED.), John Wiley & Sons, Inc., 9-130, ISBN 0-471-29406-3.

Ulaby F.T., Moore R.K. & Funk A.K. (1990). Microwave remote sensing active and passive, Norwood, M.A, Artech House, Volume III.

Wadhams P. (2002). Ice in the ocean, Gordon and Breach Science Publishers, 351p., ISBN 90-5699-296-1

Geoscience and Remote Sensing New Achievements

Edited by Pasquale Imperatore and Daniele Riccio

ISBN 978-953-7619-97-8
Hard cover, 508 pages
Publisher InTech
Published online 01, February, 2010
Published in print edition February, 2010

Our planet is nowadays continuously monitored by powerful remote sensors operating in wide portions of the electromagnetic spectrum. Our capability of acquiring detailed information on the environment has been revolutionized by revealing its inner structure, morphology and dynamical changes. The way we now observe and study the evolution of the Earth's status has even radically influenced our perception and conception of the world we live in. The aim of this book is to bring together contributions from experts to present new research results and prospects of the future developments in the area of geosciences and remote sensing; emerging research directions are discussed. The volume consists of twenty-six chapters, encompassing both theoretical aspects and application-oriented studies. An unfolding perspective on various current trends in this extremely rich area is offered. The book chapters can be categorized along different perspectives, among others, use of active or passive sensors, employed technologies and configurations, considered scenario on the Earth, scientific research area involved in the studies.

How to reference

In order to correctly reference this scholarly work, feel free to copy and paste the following:

Eric Hudier and Jean-Sebastien Gosselin (2010). Impact of Daily Melt and Freeze Patterns on Sea Ice Large Scale Roughness Features Extraction, Geoscience and Remote Sensing New Achievements, Pasquale Imperatore and Daniele Riccio (Ed.), ISBN: 978-953-7619-97-8, InTech, Available from: http://www.intechopen.com/books/geoscience-and-remote-sensing-new-achievements/impact-of-daily-melt-and-freeze-patterns-on-sea-ice-large-scale-roughness-features-extraction

INTECH
open science | open minds

InTech Europe
University Campus STeP Ri
Slavka Krautzeka 83/A
51000 Rijeka, Croatia
Phone: +385 (51) 770 447
Fax: +385 (51) 686 166
www.intechopen.com

InTech China
Unit 405, Office Block, Hotel Equatorial Shanghai
No.65, Yan An Road (West), Shanghai, 200040, China
中国上海市延安西路65号上海国际贵都大饭店办公楼405单元
Phone: +86-21-62489820
Fax: +86-21-62489821